Geografia-Malaysian Journal of Society and Space 20 issue 2 (1-23)
© 2024, e-ISSN 2682-7727 https://doi.org/10.17576/geo-2024-2002-01

Projection of rainfall distribution map under the impact of RCP4.5 and RCP8.5 climate change scenarios: A case study of Penang Island, Malaysia

Mohamed Khatif Tawaf Mohamed Yusof[1,2,] Ahmad Safuan A Rashid[1,3], Nazirah Mohd Apandi[3], Mohd Faisal Bin Abdul Khanan[4], Muhammad Zulkarnain Bin Abdul Rahman[5], Roohollah Kalatehjari[6], Afiqah Ismail[1,3], Mohd Radhie Bin Mohd Salleh[7]

[1]Department of Geotechnics and Transportation, Faculty of Civil Engineering, Universiti Teknologi Malaysia
[2]School of Civil Engineering, College of Engineering, Universiti Teknologi MARA, Johor Branch, Pasir Gudang Campus, 81750 Masai, Johor, Malaysia
[3]Centre of Tropical Geoengineering (GEOTROPIK), School of Civil Engineering, Faculty of Engineering, Universiti Teknologi Malaysia
[4]Geospatial Imaging and Information Research Group (GI2RG), Faculty of Built Environment & Surveying, Universiti Teknologi Malaysia.
[5]Tropical Resources Mapping Research Group (TropicalMap), Faculty of Built Environment & Surveying, Universiti Teknologi Malaysia
[6]Department of Built Environment Engineering, School of Future Environments, Auckland University of Technology, Auckland, 1010, New Zealand
[7]Department of Water and Environmental Engineering, Faculty of Civil Engineering, Universiti Teknologi Malaysia

Correspondence: Mohamed Khatif Tawaf Mohamed Yusof (email: mohdkhatif@uitm.edu.my)

Received: 15 October 2023; Accepted: 30 April 2024; Published: 31 May 2024

Abstract

Malaysia experiences abundant rainfall, which can potentially lead to geo-hydrological disasters. Therefore, studying the effect of climate change on rainfall events is crucial. The General Circulation Model (GCM) is a well-accepted terrestrial-scale climate simulation approach widely employed by climate scientists and researchers worldwide. However, despite its comprehensive approach, GCM lacks in necessary precision at the local level due to its coarse resolution. Consequently, employing statistical downscaling techniques becomes essential for achieving accurate simulations at the local scale. Notably, there is a scarcity of localized studies focusing on the climate change effect, specifically in Penang Island. Penang Island was selected as the study area due to its high urbanization rate and frequent geo-hydrological disasters. The current study assessed the impact of climate change on mean annual rainfall (MAR) distribution using a statistical downscaling model (SDSM) under two representative concentration pathways (RCP4.5 and RCP8.5). SDSM is calibrated and validated, and rainfall spatial distribution maps are generated through Kriging and IDW methods for the observed (1990-2019) and future (2070-2099) periods. The results indicate that under both RCPs, MAR projections increased. RCP8.5 (14.93%) shows a higher effect, where the increment percentage is almost double that of RCP4.5 (8.6%). The model displays strong correlation and performance, with a disparity of 1.24% to 11.73%, averaging 7.50%, between observed and modelled results. The outcomes of this research hold significant implications for local authorities, providing valuable insights to enhance preparedness and response strategies concerning the evolving climate conditions, particularly in

the context of geo-hydrological hazards, environmental concerns, and water security in Penang Island. However, it is crucial to acknowledge the study's limitation, considering only two climate scenarios (RCP4.5 and RCP8.5). Future research efforts should involve a broader spectrum of climate scenarios to yield a more comprehensive understanding of climate change's multifaceted and unpredictable nature for enhanced robustness of future climate-related strategies and policies.

Keywords: Climate change, Mean Annual Rainfall, Penang Island, Representative Concentration Pathway, Statistical Downscaling Model (SDSM)

Introduction

The United Nations Framework Convention on Climate Change (UNFCCC) in 1992 defines climate change as alterations in the climate system that can be attributed to human activities, either directly or indirectly. These changes can potentially impact the composition of the atmosphere and the natural variability of climate across similar periods. The World Health Organization (WHO) projected that due to the climate change effect from 2030 to 2050, there will be 250,000 deaths annually. By 2030, direct health damage costs are expected to be between 2 and 4 billion dollars annually (WHO, 2018). On top of this, Malaysia is an equatorial climate country with rainfall that varies between 2000 mm to 5000 mm annually, which might contribute to a significant climate change factor. The abundant rainfall in Malaysia benefits the country's development, such as water supply and agriculture. On the other hand, this climate condition also has negative impacts as the higher rainfall may lead to more natural disasters such as floods, landslides, and debris flow. This fact necessitates studying the effect of climate change on rainfall projection in this country (Abdul Rahman, 2018; Muhammad Nasir Mohd Adib et al., 2022; Hussain et al., 2015).

A practical way to look at climate change's effect on rainfall projection is by observing the aerosol and greenhouse gas concentrations. Several studies use GCMs to simulate a variety of aerosol concentrations and greenhouse gases or another hypothetical factors to determine their effect on the climate change phenomenon (Amin et al., 2017; Cordeiro et al., 2016; Dar et al., 2019; Sørland et al., 2018; Syafrina et al., 2017). The GCM performs well in stimulating climate change in large and terrestrial-scale climates. Unfortunately, the modelled GCM is incompatible with simulating the climate for local and site scales as its spatial resolution is too coarse (Protong et al., 2018). According to Robinson & Finkelstein (1991), the simulation of fine-scale climate change at the regional and local scale highly depends on the climate projection information details in the study area, especially in areas subjected to the complex geomorphology, islands, coasts, and regions with a high heterogeneous land surface cover.

The problem of GCM can be resolved by applying dynamical downscaling or statistical downscaling to downscale from the global scale to the regional and site scales. The Regional Climate Model (RCM) is a dynamical downscaling model useful for climate projection at the local scale involving complex local topography. According to Builes & Pántano (2021), the initial conditions for RCMs are derived from GCM simulations or dataset reanalysis. The land cover and topographical features within specific grids of GCMs are considered in the RCM to ensure that higher resolution in the diverse climatic variables is successfully simulated. The RCM not only can downscale the climate at the scale that GCM is unresolved but also improves the quality of the produced model by reducing biases associated with the driving GCM (Yang et al., 2022).

The second approach to downscaling GCM is using a statistical downscaling method. The multiple linear regression approach was used in the statistical model to downscale GCM spatial data of predictor-predict and daily relationships. The predictor variables provided daily information regarding the large-scale state of the atmosphere while the predicted variable was described at the site scale, such as rainfall and temperature (Hassan & Harun, 2011). Practically, this method has several advantages over the dynamical downscaling method. This method can offer more reliability and promises more success when dealing with tight budgets, and quick evaluations of localized climate change effects are essential (Wilby & Dawson, 2007). The Statistical Downscaling Model (SDSM) can develop a climate change scenario for the site scale at the daily time rate by statically downscaling the resolution of GCM output. Therefore, this study used SDSM to project the rainfall on the local scale in the study area under the effect of climate change.

Representative concentration pathways (RCP) refer to the simulation of various feasible global emission scenarios. RCP was created by the Intergovernmental Panel on Climate Change (IPCC) to model and explore various possible futures of greenhouse gas emissions and associated climate change impacts (IPCC, 2014). RCP describes prescribed pathways and levels of greenhouse gas concentrations for the 21st century based on varying levels of radiative forcing stabilization (Mavume et al., 2021; Vuuren et al., 2011; Vuuren & Carter, 2014).

This study employs two RCP scenarios, namely RCP 4.5 and RCP 8.5, to develop the historical and future climatic conditions for 30-year return periods (2070-2099) using the SDSM model. Both of these RCPs are widely used to represent medium stabilization (RCP4.5) and a high-emission (RCP8.5) climate scenarios in the SDSM model (Munawar et al., 2021; Mwabumba et al., 2022; Onarun et al., 2023; Protong et al., 2018; Rana & Adhikary, 2023; Zhang et al., 2020). RCP4.5 is associated with an intermediate scenario in which global emissions reach their peak in 2040 and subsequently decline. On the other hand, RCP8.5 depicts a scenario in which greenhouse gas emissions would persist in rising over the 21st century (Raymond et al., 2020).

Rainfall was expected to increase globally due to the effects of climate change. A study by Takhellambam et al. (2024) in Gulf-Atlantic coast and the Appalachian Mountains highlighted that the mean annual rainfall (MAR) was expected to increase by 7% to 36% due to the effects of climate change . There is an ongoing debate regarding the outcomes observed in previous studies concerning the future rainfall pattern in response to climate change. A study by Sa'adi et al. (2024a), Sa'adi et al. (2024b), and Sa et al. (2024) found that rainfall in Malaysia continues to show an inconsistent pattern, fluctuating under different climate change scenarios and climate zones. However, most of the zones in their study area experienced increased rainfall. Conversely, Sammathuria & Ling (2009) suggest a future reduction in Malaysia's annual rainfall due to the effects of climate change.

Limited studies have focused on the impact of climate change on Penang Island. Yang et al. (2020) tried identifying the climate change at Penang Island by utilizing rainfall data based on the interpolation method and presenting the result in a spatial distribution map. However, they did not consider the effect of climate change for future periods and only focused on the climate trend during the past period (2003-2018). Most global climate models have coarse resolutions, which may fail to represent islands' distinct topography and microclimatic variations accurately. Therefore, conducting a study focused particularly on Penang Island is imperative to provide precise and practical outcomes. In addition, the availability of rainfall stations is limited on this Island, making the spatial distribution map crucial, especially for areas that are absent or far from rainfall stations. Other than that, there is a need for research that employs downscaling techniques

to provide detailed projections and spatial rainfall distribution maps that can facilitate planning and decision-making at the local level for Penang Island.

The current study applies long-term projections (2070-2099) to assess the sustained effects of climate change on Penang Island. The long-term perspective is essential for infrastructure planning, sustainable development, and geo-hydrological hazard preparedness. The main objectives of this study, therefore, are: (1) to conduct calibration and validation of the SDSM regarding the rainfall observation record, (2) to project MAR in Penang Island under two climate change scenario (RCP4.5 and RCP8.5) for the future period 2070-2099, and (3) to develop MAR distribution map in Penang Island under the effect of climate change.

Method and Study area

Study area

Penang Island, shown in Figure 1, has been selected as the study area. It is situated between latitudes 5° 8' N to 5° 35' N and longitude 100° 8'E to 100° 32' E. According to the latest data from Malaysia (2020), Penang Island is home to approximately 825,200 residents and is considered one of the region's highest population densities, with 1691 people per square kilometre. Penang Island has been undergoing continuous development, ranging from urbanisation to agriculture. However, this rapid growth has put immense pressure on the environment, leading to various issues such as water pollution, flooding, deforestation, soil erosion, the decimation of endangered species, sedimentation, and landslides (Ahmad et al., 2006; Hassan et al., 2018). The urbanization of Penang Island can disturb its ecosystem, directly and indirectly impacting the rates of climate change on the island. Consequently, it is anticipated that climate change will significantly influence the severity and frequency of geo-hydrological hazards, given its substantial role in those phenomena.

Penang Island's MAR ranges from 2670 to 6240 mm, with the heaviest rainfall occurring during the monsoon period (Ahmad et al., 2006; Elmahdy et al., 2016). The Malaysian Meteorological Department states that Penang Island experiences a consistent surface temperature and relative humidity pattern, ranging from 27 to 35 degrees Celsius and 65% to 70%, respectively. The surface temperature of the Island reaches its highest value between April and June, while relative humidity reaches its lowest value in June, July, and September. Frequent flash floods have been reported on the Island for the past decade, and the major flood event occurred in November 2017 due to over 20 hours of rainfall**.**

Rainfall data for the study area is used as the observed data to project the rainfall for the future period. Historical rainfall data on the study area is recorded by seven rain gauge stations obtained from the Department of Irrigation and Drainage Malaysia (DID) as shown in Figure 1. The accuracy of rainfall data obtained From JPS Malaysia from the rain gauge station was within +- 0.1 mm or +-1% of the measured value (DID, 2018). Table 1 summaries the data used in the current study. This study utilizes a database spanning thirty years of mean daily rainfall data from 1991 to 2019 to project the future rainfall patterns for 2070 to 2099, employing the SDSM software. The significance of using this extensive 30-year data period lies in its importance for achieving more accurate calibration and validation results (Almazroui et al., 2017; Hasan et al., 2018; Wilby et al., 2002)**.**

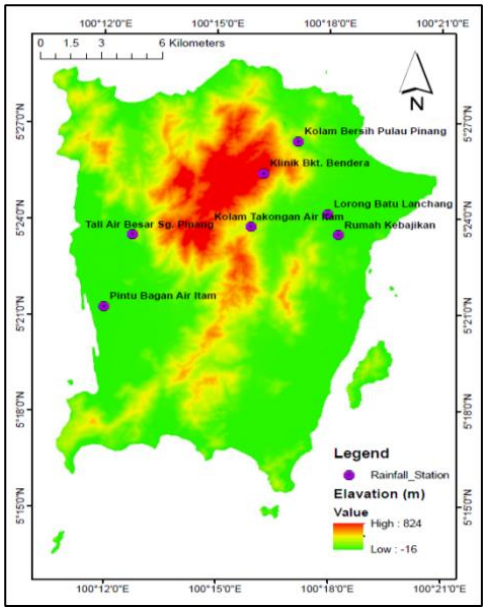

Figure 1. Study area: Penang Island

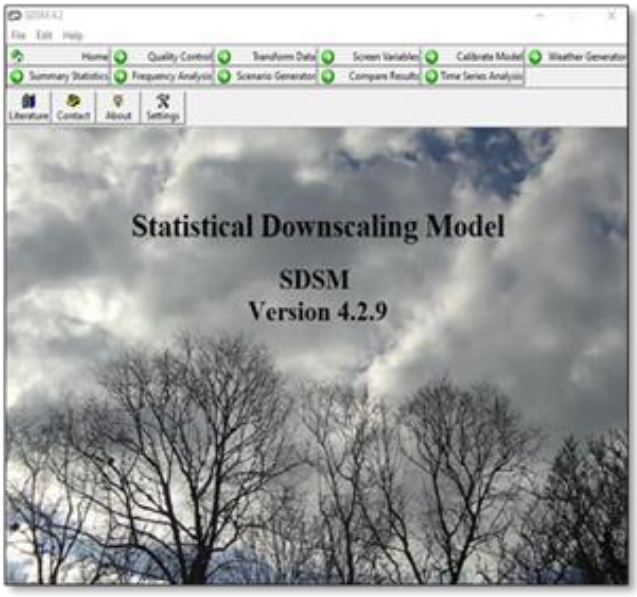

Figure 2. The interface of SDSM software

Table 1. Summary of the data used in the current study

Data type: Mean Daily Rainfall data (1991-2019)				Sources
No	Station	Latitude	Longitude	
1	Tali Air Besar Sg. Pinang	5° 23' 30"	100° 12' 45"	Department of
2	Pintu Air Bagan di Airw Itam	5° 21' 15"	100° 12' 00"	Irrigation and
3	Kolam Takongan Air Itam	5° 23' 45"	100° 15' 55"	Drainage
4	Rumah Kebajikan	5° 23' 30"	100° 18' 15"	Malaysia (JPS)
5	Klinik Bkt. Bendera	5° 25' 25"	100° 16' 15"	
6	Kolam Bersih Pulau Pinang	5° 26' 25"	100° 17' 10"	
7	Lorong Batu Lanchang	5° 24' 09"	100° 17' 58"	
Data type: Climate change scenario				
1	NCEP-NCAR_1961_2005			Canadian Centre
2	CanESM2_rcp85_2006_2100,			for Climate
3	CanESM2_rcp45_2006_2100,			Modelling and
4	CanESM2_rcp26_2006_2100			Analysis website
5	CanESM2_historical_1961_2005			(CCDS, 2020

Statistical Downscaled Model (SDSM)

In this study, SDSM software is employed, a method widely utilized in previous studies for downscaling the GCM data to the local scale (Eingrüber & Korres, 2022; El et al., 2023, 2023; Gunathilake et al., 2022; Hailu et al., 2022; Han et al., 2023; Hussain et al., 2015; Munawar et al., 2021, 2022; Onarun et al., 2023; Onarun & Sittichok, 2023; Rana & Adhikary, 2023; Zarei et al., 2023). The SDSM software comprises seven core operations, including data transformation and quality control, screening of predictor variables, model calibration, weather generation (using observed predictors), statistical analyses, visualization of model output, and scenario generation (using climate model predictors) (Wilby & Dawson, 2007). Figure 2 displays the interface of the SDSM software, and Figure 3 illustrates the overall process of climate scenario generation using SDSM. The SDSM model is calibrated using the baseline period (1990-1999) from the climate data corresponding to each station. Wilby & Dawson (2007) have authored a manual for the

SDSM software, which provides in-depth technical information regarding its application. The future global climate is significantly influenced by the level of greenhouse gases, aerosols, and other pollutants released into the atmosphere. Emission scenarios depend on these variables, creating a range of climate scenarios that account for technological advancement and socioeconomic expansion (Rianna et al., 2014).

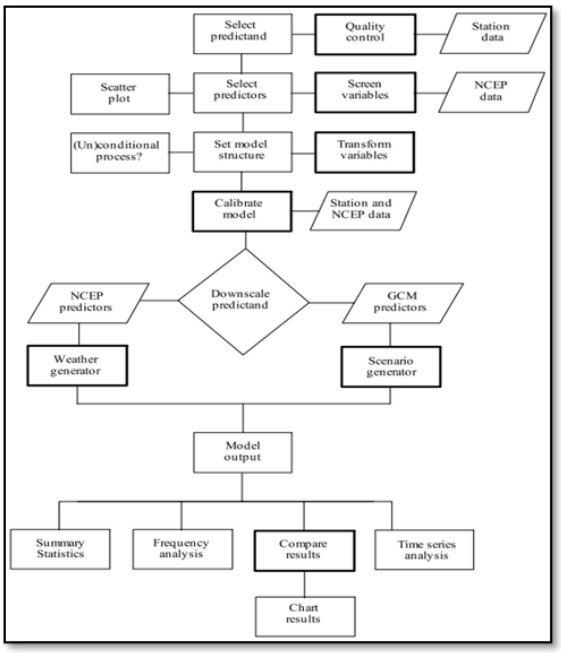

Source: Wilby & Dawson, 2007

Figure 3. Climate scenario generation using SDSM

Selection of predictor

The predictor variable used in this study is sourced from the Canadian Centre for Climate Modelling and Analysis website (CCDS, 2020), specifically, the Canadian Earth System Model known as CanESM2. The zip file is downloaded by selecting the grid box containing the selected study area, as shown in Figure 4. The downloaded file contains five primary directories, which can be extracted upon unzipping. These directories are NCEP-NCAR_1961_2005, CanESM2_rcp85_2006_2100, CanESM2_rcp45_2006_2100, CanESM2_rcp26_2006_2100, and CanESM2_historical_1961_2005. The CanESM2 directory contains 26 predictor variables used in the SDSM, as listed in Table 2.

Table 2. CanESM2 predictor variables

No	File name	Predictor names or variables	No	File name	Predictor names or variables
1	ncepmslpgl.dat	Mean sea level pressure	14	ncepp5zhgl.dat	500 hPa Divergence of true wind
2	ncepp1_fgl.dat	1000 hPa Wind speed	15	ncepp850gl.dat	850 hPa Geopotential
3	ncepp1_ugl.dat	1000 hPa Zonal wind component	16	ncepp8_fgl.dat	850 hPa Wind speed

4	ncepp1_vgl.dat	1000 hPa Meridional wind component	17	ncepp8_ugl.dat	850 hPa Zonal wind component
5	ncepp1_zgl.dat	1000 hPa Relative vorticity of true wind	18	ncepp8_vgl.dat	850 hPa Meridional wind component
6	ncepp1thgl.dat	1000 hPa Wind direction	19	ncepp8_zgl.dat	850 hPa Relative vorticity of true wind
7	ncepp1zhgl.dat	1000 hPa Divergence of true wind	20	ncepp8thgl.dat	850 hPa Wind direction
8	ncepp500gl.dat	500 hPa Geopotential	21	ncepp8zhgl.dat	850 hPa Divergence of true wind
9	ncepp5_fgl.dat	500 hPa Wind speed	22	ncepprcpgl.dat	Total precipitation
10	ncepp5_ugl.dat	500 hPa Zonal wind component	23	nceps500gl.dat	500 hPa Specific humidity
11	ncepp5_vgl.dat	500 hPa Meridional wind component	24	nceps850gl.dat	850 hPa Specific humidity
12	ncepp5_zgl.dat	500 hPa Relative vorticity of true wind	25	ncepshumgl.dat	1000 hPa Specific humidity
13	ncepp5thgl.dat	500 hPa Wind direction	26	nceptempgl.dat	Air temperature at 2 m

Source: CCDS, 2020

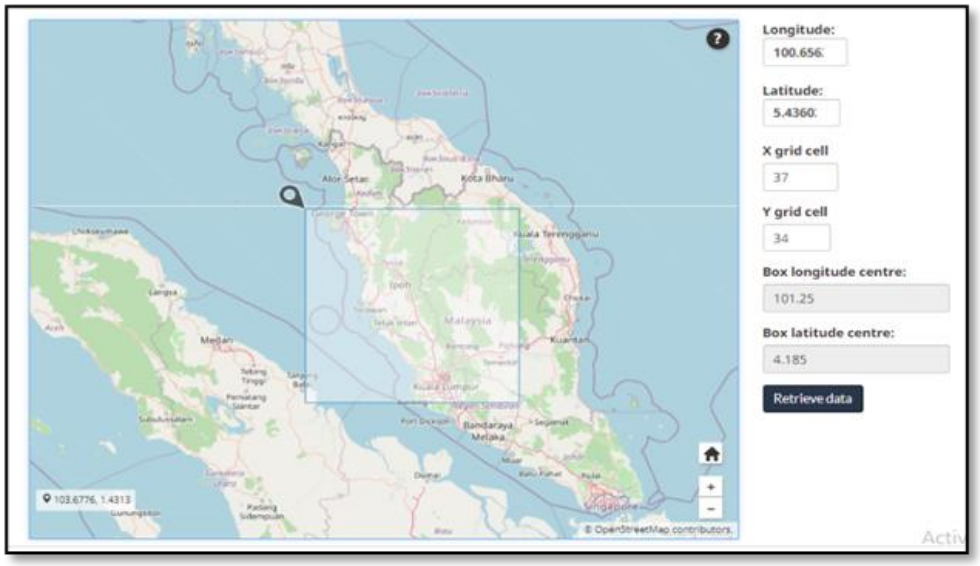

Figure 4. Zip file for downloading the CanESM2 predictor variable

The selection of variables may influence the prediction and outcome, as various atmospheric predictors can impact local variables (Hassan & Harun, 2011). In addition, the selected predictor variable must exhibit sensibility and maintain a consistent, strong correlation with the predictor, as accurately modelled by the GCM (Wilby & Dawson, 2007). The CanESM2 has been extensively employed in several studies to stimulate climate change in various study areas (Ahmadi et al., 2019; El et al., 2023; Goodarzi & Faraji, 2022; Huang et al., 2016; Mahdaoui & Asmlal, 2023; Munawar et al., 2022; Onarun et al., 2023; Onarun & Sittichok, 2023; Rana et al., 2023; Rana & Adhikary, 2023; Siabi et al., 2021; Tukimat et al., 2019; Zarei et al., 2023). Utilizing the SDSM software, the most optimal predictor variable is selected based on the analysis of linear correlation, partial correlation analysis, and scatter plots among predictor variables and predictors.

Subsequently, the MAR for each rain gauge station is generated for the future, and its distribution map is created.

Mean Annual Rainfall mapping

The results obtained from the SDSM software are integrated into ArcGIS to develop the distribution map based on the data from the seven stations within the study area. The pixel size used in ArcGIS for the study area is 10 meters, and each map contains 3,060,996 pixels, representing the total study area of 306.1 km^2. Two interpolation methods, Kriging and Inverse Distance Weighting (IDW) were employed in ArcGIS to create the MAR distribution map. Subsequently, the distribution patterns obtained from these two methods were compared for analysis. The IDW interpolation technique is widely employed as a prevalent approach for data estimates and modelling purposes, including its spatial component (Borges et al., 2016). Numerous previous studies across various fields have utilized IDW to generate different types of rainfall distribution maps (Amirabadizadeh et al., 2016; Borges et al., 2016; Hong et al., 2018; Kabiri et al., 2013; Mwabumba et al., 2022; Yang et al., 2020; Yin et al., 2019). The IDW method uses a linearly weighted dataset combination to interpolate and generate cell values for every pixel in the map. The weight is calculated based on the inverse distance between the sampled points and the point of interest (Yang et al., 2020). The surface value is interpolated based on location-dependent variables. This method assumes that the influence of a variable decreases as it is farther away from its location sampled (ESRI, 2021a).

The Kriging method computes a surface from scattered points with z-values through advanced geostatistical computations. Unlike another interpolation method in ArcGIS software, the Kriging tool stands out for its unique approach. The selection of the most effective method for developing the output surface in this method is based on considering the spatial behavior of the trend delineated by the z-values. IDWs are classified as a deterministic interpolation approach due to the smoothness of the resulting surface, determined directly from the surrounding measurements or specified mathematical formulas (ESRI, 2021b). On the other hand, Kriging presents the second classification of interpolation methods using the Geostatistical principle. This method is developed through statistical models incorporating autocorrelation or the statistical relationship between measured points. Consequently, geostatistical methods can provide prediction surfaces and offer prediction accuracy assessments. In the Kriging method, the output value for any location is subjected to a mathematical function tailored to the specific number or radius within the dataset. Kriging method is widely recognized as one of the standard methods used to develop variations of the rainfall distribution map across diverse research areas (Borges et al., 2016; Chen et al., 2019; Hu et al., 2020; Shou et al., 2018; Tukimat et al., 2019; Yendra et al., 2017).

Results and discussion

Validation of model

The calibration of the SDSM model is conducted using a multiple regression equation, which is developed using atmospheric variables (the predictors) and daily weather data (the predictand) (Wilby & Dawson, 2007, 2015). The downscaling model for monthly rainfall at each station is developed using the predictor variables selected from the CanESM2 dataset. As per Hassan &

Harun (2011), a high correlation value is indicated by a strong correlation between predictors and predictands across all twelve months. The baseline period for the current study is established using the rainfall dataset collected from seven rain gauge stations within the study area, spanning period from 1990 to 2019. This baseline period is then subsequently divided into two distinct parts: the calibration period, covering the years 1990 to 1999, and the validation period, spanning from 2000 to 2019. Based on the observed time series data inputs, the validation process generates synthetic daily weather data and multiple linear regression parameters. Notably, these parameters were not employed during the calibration phase. The summary of the comparison between observed and modelled annual rainfall is summarized in Table 3. The evaluation of environmental model performance can be conducted using various statistical indices, as outlined in the study by Bennett et al. (2013). These indices include Mean Absolute Error (MAE) and Root Mean Square Error (RMSE). This study validated the model's performance using the mentioned statistical index. The MAE and RMSE were calculated based on Equations 1 and 2.

$$RMSE = \sqrt{\frac{1}{n}\sum_{i=1}^{n}(X_{predicted} - X_{actual})} \quad (1)$$

$$MAE = \frac{1}{n}\sum_{i=1}^{n}\left|X_{predicted} - X_{actual}\right| \quad (2)$$

Table 3. Comparison of observed and modelled rainfall for the validation phase (2000-2019)

Station	Tali Air Besar Sg. Pinang		Pintu Bagan Air Itam		Kolam Takongan Air Itam		Rumah Kebajikan	
Month	**O**	**M**	**O**	**M**	**O**	**M**	**O**	**M**
Jan	201.7	93.4	216.8	117.3	194.4	68.2	128.8	43.2
Feb	151.1	88.3	171.6	64.3	170.9	65.5	134.4	45.7
Mar	181.7	157.9	204.9	177.2	163.6	129.7	132.5	80.2
Apr	179.9	228.0	175.2	203.3	160.0	137.0	135.8	141.6
May	211.8	216.8	219.6	236.8	151.4	157.4	156.8	172.8
Jun	201.5	176.3	194.0	166.2	176.2	161.9	134.0	117.9
Jul	202.2	226.0	232.8	176.3	192.4	204.8	178.7	193.5
Aug	201.5	278.1	198.7	220.9	161.3	284.1	175.6	184.9
Sep	203.9	343.3	190.4	365.0	172.0	240.3	152.8	305.6
Oct	205.6	389.1	264.3	358.0	187.2	299.3	163.7	337.4
Nov	206.3	298.4	216.2	240.2	175.8	373.8	160.2	125.5
Dec	222.2	141.3	251.2	104.4	164.1	112.5	145.7	73.0
Total	**2369**	**2637**	**2536**	**2430**	**2069**	**2234**	**1799**	**1821**
% of differences	**11.3**		**4.2**		**8.0**		**1.2**	
MAE	**72.5**		**68.8**		**72.8**		**60.2**	
RMSE	**88.4**		**86.2**		**92.8**		**81.0**	

Station	Klinik Bkt. Bendera		Kolam Bersih Pulau Pinang		Lorong Batu Lanchang	
Month	**O**	**M**	**O**	**M**	**O**	**M**
Jan	215.3	73.3	177.8	69.6	166.9	103.1
Feb	180.2	80.5	159.2	72.3	137.7	69.8

Mar	190.3	146.9	168.9	153.0	174.8	124.9
Apr	215.6	214.4	173.4	172.0	175.9	173.5
May	162.3	202.9	198.8	195.7	183.8	212.3
Jun	183.5	179.5	198.5	186.5	177.0	157.1
Jul	174.6	234.0	185.5	231.0	152.2	164.5
Aug	188.8	267.3	172.3	280.2	215.5	229.0
Sep	193.2	375.0	166.2	340.1	181.7	326.6
Oct	215.3	332.5	201.3	319.9	181.6	342.2
Nov	188.1	327.7	206.6	229.3	190.5	260.8
Dec	212.1	157.2	166.3	120.1	184.7	110.1
Total	**2319**	**2591**	**2175**	**2370**	**2122**	**2274**
% of differences	**11.7**		**9.0**		**7.1**	
MAE	**80.2**		**61.9**		**59.1**	
RMSE	**96.9**		**81.8**		**76.4**	

*O=Observed
M=Modelled

The result revealed a satisfactory agreement between the observed and modelled annual rainfall at the seven stations. The observed and modelled data disparity ranged from approximately 1.24% to 11.73%, with an average deviation of 7.50%. Specifically, the model yielded average values of 67.91 mm/month and 86.21 mm/month, falling within the range of 59.1-80.2 mm/month and 59.1-76.4 mm/month for MAE and RMSE, respectively. During the validation period, the highest and lowest errors between the modelled and observed MAR occurred at the Klinik Bukit Bendera and Lorong Batu Lanchang stations, respectively. The Klinik Bukit Bendera station is at the highest elevation among all the stations.

In contrast, the Lorong Batu Lanchang station is at the third-lowest elevation, 8 meters above sea level. Pintu Bagan Air Hitam has the lowest elevation but recorded the highest MAR observation. However, this station exhibited a unique pattern where the modelled MAR was smaller than the observed, deviating from the general observed at other stations. All the other stations displayed a consistent pattern where the modelled MAR exceeded the observed value.

Rainfall Projection under Climate Change

The GCM projections are determined by the RCP framework (Moss et al., 2010). The future climatic conditions are simulated using the SDSM model under two different RCP scenarios: RCP 4.5 and RCP 8.5 for 30-year return periods (2070-2099). The RCP 4.5 scenario considers utilizing technology and strategies to reduce greenhouse gas emissions to stabilize the total radiative forcing before 2100. Conversely, the RCP 4.5 scenario projects climate change, assuming that carbon dioxide emissions are maintained at the current rate (Kim et al., 2015). Under the RCP 8.5 scenario, greenhouse gas concentrations and radiative forcing levels are simulated at their highest levels. Kim et al. (2015) clarify that in RCP 8.5, the climate is projected, assuming that current carbon dioxide emission levels undergo drastic changes. The comparison between observed MAR and modelled MAR for the future period under RCP 4.5 and RCP 8.5 for the seven stations is illustrated in Figure 5 (a-g**)** and summarized in Table 4.

Overall, the modelled MAR is projected to increase (2070-2099) under RCP4.5 and RCP8.5 scenarios. This finding aligns with the study conducted by Lal et al. (2012), where they observed a similar increase in annual rainfall in the future within the northern mid-latitudes, a correlation with the study area. The observational results for the period (1990-2019) indicated that

the Pintu Bagan Air Hitam station had the highest MAR value, while the Rumah Kebajikan Station had the lowest value. The average value of the observed MAR for all the stations is 2350.256 mm. Notably, only the Rumah Kebajikan station recorded a MAR value below 2000 mm, whereas all the other stations exhibited values exceeding 2000 mm. Under RCP4.5, all the stations are projected to receive a MAR of more than 2100 mm, with an average value of 2555.29 mm. The Klinik Bukit Bendera station is expected to receive the highest MAR, while the Kolam Takungan Air Itam station indicated the lowest value for both RCP conditions in the future. Under RCP8.5, all the stations are anticipated to receive a MAR of more than 2200 mm, with an average value of 2701.091mm.

In general, the future rainfall changes range between 4.76% and 33.36%, with an average change of 8.6% under RCP 4.5 and 14.93% under RCP 8.5. The future rainfall in Peninsular Malaysia will change from -6% to +11% (NAHRIM, 2013). Three stations, namely Rumah Kebajikan, Klinik Bukit Bendera, and Kolam Bersih Pulau Pinang showed an increase of more than 11% in future rainfall under both RCP scenarios. All the remaining stations exhibited a notable change in MAR in alignment with the findings of NAHRIM (2013), except for the Tali Air Besar Sg Pinang Station. The Tali Air Besar Sg Pinang station experienced a MAR increment of more than 11% under RCP8.5. Notably, the MAR projections under RCP4.5 and RCP8.5 indicated increased rainfall for the future (2070-2099) across all the stations, except for The Pintu Bagan Air Hitam. This is surprising given the fact that Pintu Bagan Air Hitam had experienced the highest MAR value during the observation period. Indeed, Pintu Bagan Air Hitam displayed a deviating pattern during the validation phase, being the sole station where the observed MAR exceeded the modelled value. In addition, it exhibited the highest observed MAR value for the calibration period.

Kolam Bersih Pulau Pinang Station exhibited the highest increment value for the future period, while MAR for Pintu Bagan Air Itam Station is anticipated to decrease slightly under both RCPs. Surprisingly, the observed amount did not significantly influence the percentage increment of MAR for the future period under RCP4.5 and RCP 8.5. For instance, Pintu Bagan Air Itam Station had the highest observed value, but the projection was the lowest for both RCP types in the future period. Most stations indicated a higher percentage of rainfall change under RCP 8.5 than under RCP 4.5. The exceptions were Kolam Takongan Air Itam and Lorong Batu Lanchang stations, which displayed almost similar increment percentages of MAR, differing by less than 0.4% under both RCPs.

The predictions made by Lal et al. (2012) indicated that extreme weather conditions are likely to cause significant alterations in both rainfall intensity and seasonality due to the expected rise in extreme weather events. This study concurs with these findings, suggesting a projected increase in rainfall levels by approximately 70-600 mm annually across Penang Island. However, it is noteworthy that the Pintu Air Bagan Air Itam station is anticipated to experience a reduction in MAR by 90-120 mm. Similar trends of increased rainfall in the future were also observed in studies conducted by Syafrina et al. (2017) and Tan et al. (2017). Conversely, the Malaysian Meteorological Department (2009) and Sammathuria & Ling (2009) predicted a future reduction in MAR for Malaysia, introducing an element of inconsistency and uncertainty regarding future rainfall patterns. This variability aligns with the findings of Abdul Rahman (2018) and Tang (2019), emphasizing that future rainfall patterns exhibit inconsistency in pattern concentration and quantity. These disparities underline the complexity and uncertainties of predicting future weather patterns, particularly in changing climate conditions.

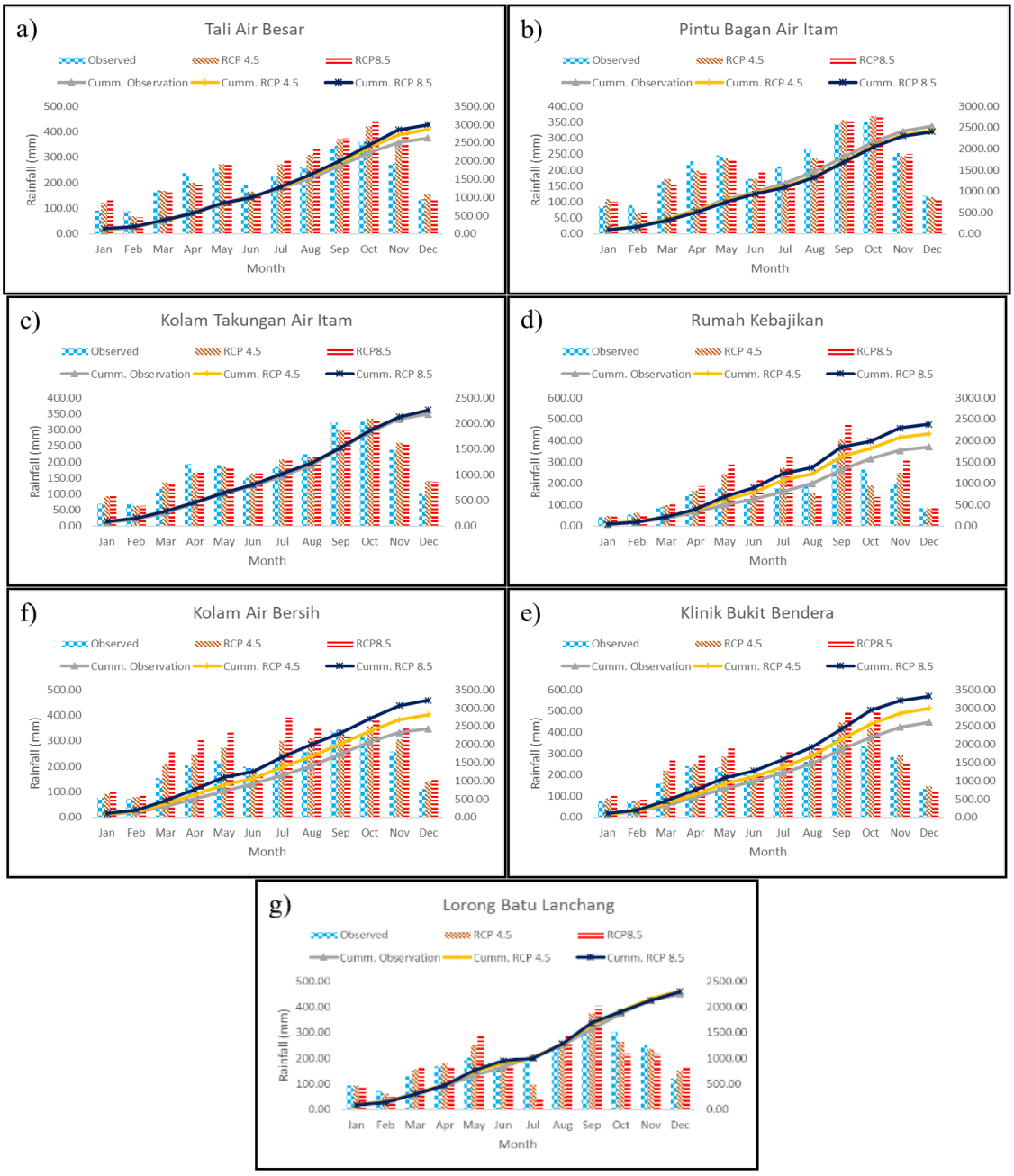

Figure 5. Mean monthly rainfall for observed (1990-2019) and modelled future period (2070-2099) under RCP 4.5 and RCP 8.5: (a) Tali Air Besar Sg. Pinang, (b) Pintu Bagan Air Itam, (c) Kolam Takongan Air Itam, (d) Rumah Kebajikan, (e) Klinik Bkt. Bendera, (f) Kolam Bersih Pulau Pinang, and (g) Lorong Batu Lanchang.

Rainfall modelling is an inherently complex task due to the involvement of conditional processes influenced by intermediary factors, such as humidity and cloud cover. Several studies have highlighted the complexity of downscaling rainfall data (Hassan & Harun, 2011). The intricate nature of these processes raises questions about the reliability of projected rainfall patterns in response to climate change, as evidenced by discrepancies observed in previous studies. The uncertainties in predicting future weather events derive from the limitations of the model in capturing periodic ocean-atmospheric oscillations, notably the Indian Ocean Dipole (IOD) and

extreme weather events such as La Niña and El Niño, which are linked with the past extreme weather events (Tang, 2019).

Table 4. Comparison of observed and modelled rainfall for the future period

No	Station	Elevation (m)	Average Annual Rainfall (mm)			% of increment	
			Observed (1990-2019)	RCP 4.5 (2070-2099)	RCP 8.5 (2070-2099)	RCP 4.5 (2070-2099)	RCP 8.5 (2070-2099)
1	Tali Air Besar Sg. Pinang	51	2635.593	2876.587	3000.677	9.14382	13.85204
2	Pintu Bagan Air Itam	0	2529.517	2438.127	2409.216	-3.61291	-4.75586
3	Kolam Takongan Air Itam	205	2195.4	2266.543	2264.843	3.240541	3.163112
4	Rumah Kebajikan	7	1788.273	2157.79	2385.072	20.66334	33.37295
5	Klinik Bkt. Bendera	626	2611.87	2997.761	3331.33	14.77452	27.5458
6	Kolam Bersih Pulau Pinang	52	2437.003	2820.419	3216.127	15.73308	31.97055
7	Lorong Batu Lanchang	8	2254.135	2308.806	2300.375	2.42537	2.05134
Average			**2350.256**	**2552.29**	**2701.091**	**8.596283**	**14.92755**

Mean Rainfall Distribution map

The rainfall distribution map for the observation period and the future period under RCP 8.5 and RCP 4.5 is shown in Figure 6**,** and its comparison is summarized in **Table 5**. The distribution map of MAR for the observation period (1990-2019) indicated minimal differences in average mean values, with slight variations in minimum and maximum values between the Kriging and IDW methods. Compared to the MAR values projected for rainfall under RCP 4.5 and RCP 8.5 for the future period (2070-2099), all mean, minimum, and maximum values showed minimal disparities, remaining below 1%. The MAR distribution map for the observation period indicated that the study area received almost 40% of the rainfall within the 2400-2500 mm range for both interpolation methods. Three predominant MAR classes ranging from 2200-2500mm constituted a cumulative 92.44% and 75.75% of the study area for the observation period under the Kriging and IDW methods, respectively. However, these dominant classes are expected to decrease in the future drastically. The cumulative percentage of the area covered by these classes is projected to decrease by 2.85% to 38.41%, with the 2400-2500 mm class showing the highest reduction. This signals a significant shift in the rainfall distribution pattern, indicating the impact of climate change on the region's rainfall levels.

The MAR is predicted to increase for both RCPs based on the map shown in Figure 6. The areas receiving MARs of more than 2500 mm will undergo drastic changes, with 87.73% (Kriging) and 61.2% (IDW) of the study expected to receive MAR exceeding 2500 mm under RCP 4.5. Furthermore, under RCP 8.5, even greater changes are anticipated, with 94.43% and 91.3% for the Kriging and IDW methods, respectively. Both the Kriging and IDW methods comprise a similar number of MAR classes, but the distribution area varies for each class under both RCPs. Specifically, under the Kriging method for RCP 4.5, a significant portion of the area (69.36%) is projected to receive 2500-2600 mm of MAR.

Conversely, under IDW, this rainfall class only represents 23.83% of the area, whereas the highest class is 2400-2500 mm, representing 25.37 % of the study area. The dominant mean rainfall class with the Kriging method will shift to 2500-2600 mm and 2700-2800 mm for RCP 4.5 and RCP 8.5, respectively. This single class represents almost 65% of the rainfall distribution in the future for both RCPs with the Kriging method, which contrasts with the IDW method. Rainfall is spread across several dominant classes to create a more even distribution pattern.

Table 5. Comparison of mean annual rainfall distribution using Kriging and IDW method for observation and future period

Mean Annual Rainfall (mm)	Observation (1990-2019)			RCP 4.5 (2070-2099)			RCP8.5 (2070-2099)		
	Kriging Area (km)	IDW Area (km)	Different (%)	Kriging Area (km)	IDW Area (km)	Different (%)	Kriging Area (km)	IDW Area (km)	Different (%)
1700-1800	NA	0.11 (0.04%)	-0.04		NA			NA	
1800-1900		1.51 (0.49%)	-0.49						
1900-200		3.87 (1.26%)	-1.26						
2000-2100	0.06 (0.02%)	7.84 (2.56%)	-2.54						
2100-2200	17.95 (5.86%)	20.4 (6.66%)	-0.8	0.29 (0.09%)	1.18 (0.39%)	-0.29			
2200-2300	40.82 (13.34%)	51.28 (16.75%)	-3.42	3.48 (1.14%)	9.57 (3.13%)	-1.99	0.15 (0.05%)	0 (0.00%)	0.05
2300-2400	115.14 (37.615)	64.95 (21.22%)	16.4	12.34 (4.03%)	30.34 (9.91%)	-5.88	4.46 (1.46%)	0.69 (0.23%)	1.23
2400-2500	127 (41.495)	115.64 (37.78%)	3.71	21.44 (7.01%)	77.65 (25.37%)	-18.36	12.42 (4.06%)	8.01 (2.62%)	1.44
2500-2600	5.13 (1.68%)	36.22 (11.83%)	-10.16	212.32 (69.36%)	72.95 (23.83%)	45.53	17.9 (5.85%)	32.92 (10.75%)	-4.91
2600-2700	NA	4.29 (1.40%)	-1.4	33.42 (10.92%)	56.18 (18.35%)	-7.43	33.93 (11.08%)	94.76 (30.96%)	-19.87
2700-2800		NA		14.5 (4.74%)	43.03 (14.06%)	-9.32	199.31 (65.11%)	52.81 (17.25%)	47.86
2800-2900				6.58 (2.15%)	13.08 (4.27%)	-2.12	18.7 (6.11%)	13.54 (4.42%)	1.68
2900-3000				1.73 (0.56%)	2.11 (0.69%)	-0.13	8.61 (2.81%)	49.32 (16.11%)	-13.3
3000-3100					NA		4.26 (1.39%)	41.92 (13.69%)	-12.3
3100-3200							3.6 (1.18%)	9.26 (30.2%)	-1.85
3200-3300							2.61 (0.85%)	2.45 (0.80%)	0.05
3300-3400							0.17 (0.05%)	0.43 (0.14%)	-0.09
Min	**2094.51**	**1788.28**	**14.62**	**2158.31**	**2157.79**	**0.02**	**2265.43**	**2264.84**	**0.03**
Mean	**2374.76**	**2364.91**	**0.41**	**2570.56**	**2554.35**	**0.63**	**2714.28**	**2691.53**	**0.84**
Max	**2523.64**	**2635.59**	**-4.44**	**2997.31**	**2997.76**	**-0.01**	**3330.75**	**3331.33**	**-0.02**

Various maps have been published, illustrating the projected rainfall and temperature for the future (Amirabadizadeh et al., 2016; Kabiri et al., 2013; Lim et al., 2009; Pour et al., 2014). These maps provide valuable insights into how rainfall patterns evolved, notably in response to increased human activity during the twentieth century. The correlation between these changes and anthropogenic activities, which lead to higher aerosol concentration and the greenhouse effect,

contributes to a projected increase in rainfall in the future. The output of the SDSM for two distinct RCPs consistently points in the same direction. It anticipates significant alterations in rainfall distribution, with an overall rise in MAR. However, the increase in rainfall under RCP 8.5 is notably higher. This is the importance of greenhouse gas concentration and radiative forcing levels, simulated at their peak under RCP 8.5, reflecting drastic shifts in current carbon dioxide emissions. Conversely, the greenhouse effect is anticipated to decrease, assuming carbon dioxide emissions remain stable at current rates under RCP 4.5, owing to technological advancements and policy implementations.

The study's findings underscore the substantial differences between the two RCP scenarios. The average increment in rainfall is 8.6% for RCP 4.5 and 14.9% for RCP 8.5, as detailed in Table 4. Notably, the percentage increment in rainfall under RCP 4.5 is nearly half of that projected under RCP 8.5. Consequently, the distribution of MAR in Penang Island is markedly altered under RCP 8.5, with a substantial increase in areas receiving higher rainfall. These insights illuminate the critical impact of greenhouse gas emissions scenarios on regional climate patterns, providing crucial information for informed decision-making and adaptive strategies.

Syafrina et al. (2017)) used the Advanced Weather Generator model as a climate model and found out that hourly and 24-hour extreme rainfall in Malaysia was expected to increase during the projection period (2081-2100) with a wider spatial distribution under the RCP 6.0 scenario. Tan et al. (2017) also found the same trend, where the projection of MAR using GCM shows an increment under RCP 2.6, 4.5, and 8.5 climate scenarios. Another study by Adib & Harun (2022) utilized a machine learning approach and found that monthly rainfall was projected to increase under three different shared socioeconomic pathways (SSPs). All those findings show a significant trend compared to the results of the current study. However, a report by the Malaysian Meteorological Department (2009) shows contradictory findings where Malaysia's annual rainfall modelled using the PRECIS regional climate model was predicted to reduce radically in the future period. These uncertainties were significant to the findings by Abdul Rahman (2018) and Tang (2019), who highlighted that rainfall continuously shows an inconsistent pattern in the future with variations in concentration and amount.

The changes in the MAR pattern under the effect of climate change lead to more frequent floods, which is a crucial challenge for water resources management. Climate change can heighten the vulnerability of water infrastructure, including dams, levees, and irrigation systems, to severe weather phenomena such as floods, storms, and landslides. These might undermine water resources management. Adaptive water management systems must be developed and put into practice in response to climate change in order to deal with the increment of rainfall intensity (Noor et al., 2018). This includes making investments in water-efficient technology, enhancing water distribution and storage infrastructure, and restoring natural ecosystems that control the quantity and quality of water available. In addition, the effects of climate change on water resources can be mitigated by maintaining and restoring natural ecosystems, such as riparian zones, wetlands, and forests. These natural ecosystems can improve water quality, control water flows, and encounter the erosion and sedimentation effect due to increasing rainfall. The current study's projection can be utilized for long-term planning and decision-making processes for efficient water resources management in response to climate change.

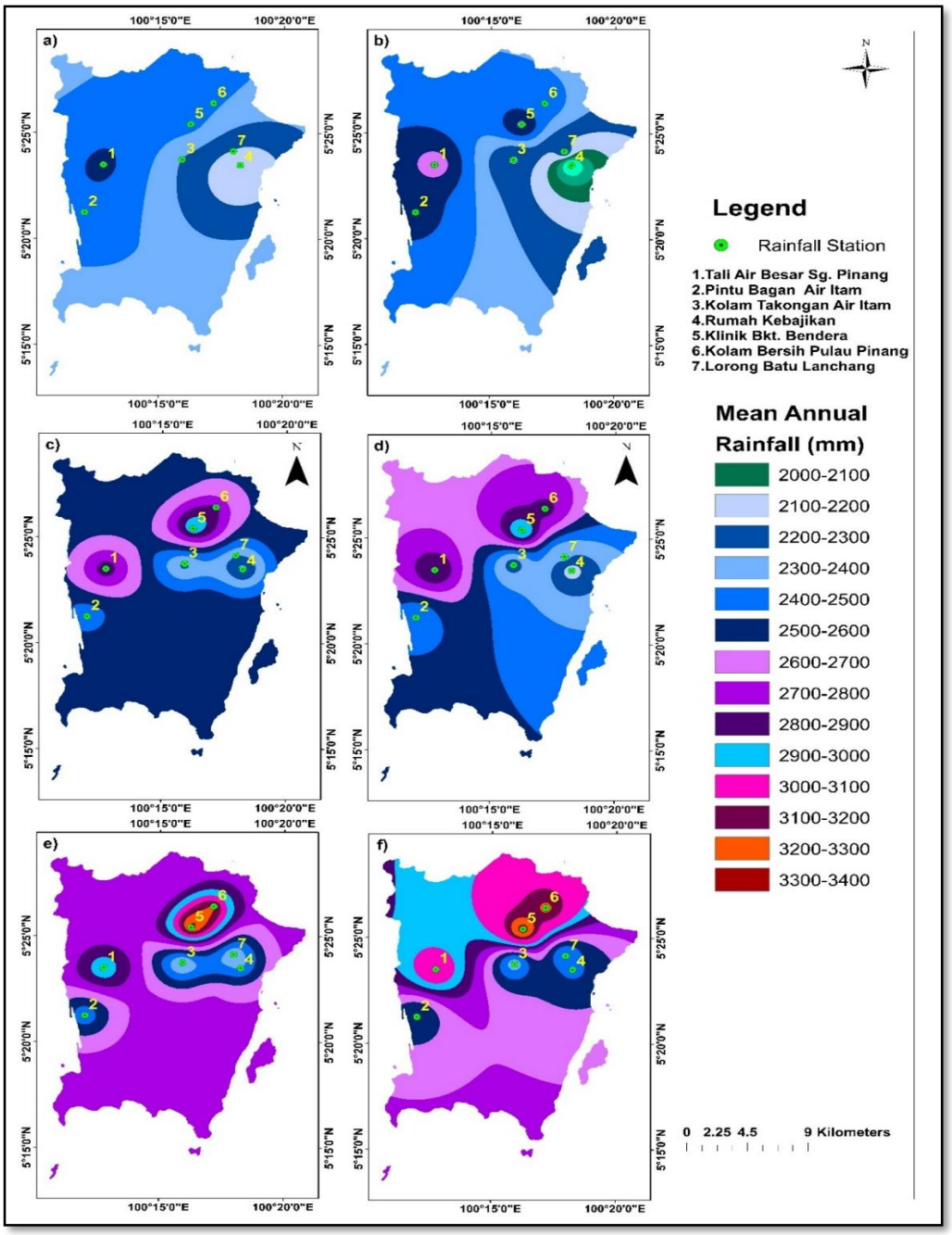

Figure 6. Mean Annual Rainfall Distribution Map Under: a) Observation (Kriging); b)Observation (IDW); c)RCP4.5 (Kriging); d)RCP4.5 (IDW); e)RCP8.5 (Kriging); f)RCP8.5 (IDW)

Conclusion

The SDSM model, developed using data from the seven observation stations, underwent rigorous validation and comparison with observed data, resulting in a notable agreement with a disparity ranging from 1.24% to 11.73%, averaging 7.50%. This significant correlation between predictors

and selected predictors underscores the robust performance of the developed SDSM model.

The study successfully projected MAR for the future (2070-2099) under two emission scenarios: RCP 4.5 and RCP 8.5. The findings indicate a consistent increase in rainfall in the future under both RCP conditions. However, MAR under RCP 8.5 demonstrates a substantially higher increment, nearly twice that under RCP 4.5. This emphasizes the critical importance of considering RCP 8.5, given the continuous rise in emissions. Understanding and preparing for this worst-case scenario is paramount, as it represents the higher end of possible climate change impacts. Stakeholders must implement strategies to address the significant changes anticipated under RCP 8.5.

The study also generated rainfall distribution maps, revealing expected changes in rainfall patterns. Under the Inverse Distance Weighting (IDW) method, rainfall distribution appears more uniform, with less dominance of specific rainfall classes than the Kriging method. In the future, areas receiving MAR above 2500 mm will increase significantly, ranging from 61.2% to 94.43%. Notably, the Kriging method exhibits a higher percentage of distribution value increment than IDW under both RCP conditions.

These findings underscore the urgency for comprehensive climate change adaptation strategies, emphasizing the need to prepare for intensified rainfall scenarios, especially under the RCP 8.5 emissions trajectory. Such preparedness ensures that mitigation efforts are aligned with the most challenging climate change scenarios, fostering resilience and sustainability in evolving climate patterns.

The anticipated increase in rainfall in the future could potentially trigger severe environmental disasters such as floods, landslides, and debris flows. The study's findings have been effectively transformed into visual representations, including graphs, tables, and maps, facilitating easy interpretation to enhance the understanding of these projections. Local authorities and relevant stakeholders in Penang Island could leverage the insights from this study to maintain their preparedness and response strategies in the face of climate change. The study is a foundational resource for exploring the intricate relationship between climate change and its diverse impacts, including geo-hydrological hazards, environmental shifts, and water security on the Island.

However, it is essential to acknowledge the uncertainties inherent in climate change projections. Future studies should encompass a broader spectrum of climate scenarios to address these uncertainties comprehensively. While the current study focused on RCP4.5 and RCP8.5, incorporating other relevant emission scenarios like socioeconomic pathways 126, 245, 370, and 585 would provide a more thorough understanding of potential climate variations. Additionally, enhancing the study's spatial representation by increasing the number of rainfall stations across different parts of Penang Island is advisable. This expansion would improve the accuracy and performance of rainfall distribution maps developed through interpolation methods in ArcGIS. By considering these recommendations in future research endeavors, a more robust and detailed understanding of the region's climate dynamics and associated hazards can be attained, aiding in more effective climate adaptation and mitigation strategies.

Acknowledgment

This project was technically and financially supported by Universiti Teknologi Mara (UiTM) Cawangan Johor Kampus Pasir Gudang and Universiti Teknologi Malaysia (UTM). This project is also funded by the UTM Matching Grant: Vote Q.J130000.3052.04M26). The Department of Irrigation and Drainage Malaysia, (DID) Malaysia provided the daily rainfall data.

References

Abdul Rahman, H. (2018). Climate change scenarios in Malaysia: Engaging the public. *International Journal of Malay-Nusantara Studies, 1*(2), 55–77.

ABed, S. S. (2021). Future climate projections in Algeria using statistical downscaling model. *Research Square,* 1-28.

Adib, M. N. M., & Harun, S. (2022). Metalearning approach coupled with CMIP6 Multi-GCM for future monthly streamflow forecasting. *Journal of Hydrologic Engineering, 27*(6).

Adib, Muhammad Nasir Mohd, Harun, S., & Rowshon, M. K. (2022). Long-term rainfall projection based on CMIP6 scenarios for Kurau River Basin of rice-growing irrigation scheme, Malaysia. *SN Applied Sciences, 4*(70).

Ahmadi, M., Motamedvaziri, B., Ahmadi, H., Moeini, A., & Zehtabiyan, G. R. (2019). Assessment of climate change impact on surface runoff, statistical downscaling and hydrological modeling. *Physics and Chemistry of the Earth*, *114*, 102800.

Almazroui, M., Islam, M. N., Balkhair, K. S., Şen, Z., & Masood, A. (2017). Rainwater harvesting possibility under climate change: A basin-scale case study over western province of Saudi Arabia. *Atmospheric Research*, *189*, 11–23.

Amin, M. Z. M., Shaaban, A. J., Ercan, A., Ishida, K., Kavvas, M. L., Chen, Z. Q., & Jang, S. (2017). Future climate change impact assessment of watershed scale hydrologic processes in Peninsular Malaysia by a regional climate model coupled with a physically-based hydrology modelo. *Science of the Total Environment*, *575*, 12–22.

Amirabadizadeh, M., Ghazali, A. H., Huang, Y. F., & Wayayok, A. (2016). Downscaling daily precipitation and temperatures over the Langat River Basin in Malaysia : A comparison of two statistical downscaling approaches. *International Journal of Water Resources and Environmental Engineering*, *8*, 120–136.

Bennett, N. D., Croke, B. F. W., Guariso, G., Guillaume, J. H. A., Hamilton, S. H., Jakeman, A. J., Marsili-Libelli, S., Newham, L. T. H., Norton, J. P., Perrin, C., Pierce, S. A., Robson, B., Seppelt, R., Voinov, A. A., Fath, B. D., & Andreassian, V. (2013). Characterising performance of environmental models. *Environmental Modelling and Software*, *40*, 1–20.

Borges, P., Franke, J., Anunciação, Y. M. T., Weiss, H., & Bernhofer, C. (2016). Comparison of spatial interpolation methods for the estimation of precipitation distribution in Distrito Federal, Brazil. *Theoretical and Applied Climatology*, *123*, 335–348.

Builes-Jaramillo, A., & Pántano, V. (2021). Comparison of spatial and temporal performance of two Regional Climate Models in the Amazon and La Plata river basins. *Atmospheric Research*, *250*, 105413.

CCDS. (2020). Canadian climate data and scenarios. https://climate-scenarios.canada.ca/

Cordeiro Pires, A., Nolasco, R., Rocha, A., Ramos, A. M., & Dubert, J. (2016). Climate change in the Iberian Upwelling System: A numerical study using GCM downscaling. *Climate Dynamics, 47*, 451–464.

Dar, M. U. D., Aggarwal, R., & Kaur, S. (2019). Climate predictions for Ludhiana district of Indian Punjab under RCP 4.5 and RCP 8.5. *International Journal of Environment and Climate Change, 8*(2), 128-141.

Eingrüber, N., & Korres, W. (2022). Climate change simulation and trend analysis of extreme precipitation and floods in the mesoscale Rur catchment in western Germany until 2099 using Statistical Downscaling Model (SDSM) and the Soil & Water Assessment Tool (SWAT model). *Science of the Total Environment, 838*(1), 155775.

El Hafyani, M., Essahlaoui, N., Essahlaoui, A., Mohajane, M., & Van Rompaey, A. (2023). Generation of climate change scenarios for rainfall and temperature using SDSM in a Mediterranean environment: A case study of Boufakrane river watershed, Morocco. *Journal of Umm Al-Qura University for Applied Sciences*, *9*, 436-448.

ESRI. (2021a). IDW - Help | ArcGIS for Desktop. https://desktop.arcgis.com/en/arcmap/10.3/tools/3d-analyst-toolbox/idw.htm

ESRI. (2021b). Kriging—Help | ArcGIS for Desktop. https://desktop.arcgis.com/en/arcmap/10.3/tools/3d-analyst-toolbox/kriging.htm

Goodarzi, M., & Faraji, A. (2022). Analysis of Low-Flow Indices in the Era of climate change: An application of CanESM2 model. In U. Chatterjee, A. O. Akanwa, S. Kumar, S. K. Singh, & A. Dutta Roy (Eds.), *Ecological footprints of climate change : Adaptive approaches and sustainability* (pp. 95–115). Springer International Publishing.

Gunathilake, M. B., Samarasinghe, H. D. J. T., Bandara, I., & Chathuranika, I. (2022). Analysis of Statistical Downscaling Model (SDSM) projected future rainfall in Northwestern, Western and Southern provinces of Sri Lanka Analysis of Statistical Downscaling Model (SDSM) projected future rainfall in Northwestern, Western and Southern. *Ruhuna Journal of Science*, *13*(1), 70–91.

Hailu, M., Mishra, S., Jain, S., & Singh, V. (2022). Evaluation and application of SDSM to assess the projected climate change effects on the Tekeze watershed, Ethiopia. *Modeling Earth Systems and Environment*, *9*, 1275-1285.

Han, Y., Yang, J., & Das, L. C. (2023). Evaluation of Sdsm Models for Climate Predictions in Bangladesh. *International Journal of Big Data Mining for Global Warming*, *5*(1), 235003.

Hasan, D., Ratnayake, U., Shams, S., Nayan, Z., & Rahman, E. (2018). Prediction of climate change in Brunei Darussalam using statistical downscaling model. *Theoretical and Applied Climatology*, *133*(3), 343-360.

Hassan, Z., & Harun, S. (2011). *Hydrological response of a catchment to climate change in the Kurau River Basin , Perak , Malaysia.* 3rd International Conference on Managing Rivers in the 21st Century: Sustainable solutions for global crisis of flooding, pollution and water scarcity (pp. 216-225), 6th - 9th December, Penang, Malaysia.

Hong, H., Liu, J., Bui, D. T., Pradhan, B., Acharya, T. D., Pham, B. T., Zhu, A. X., Chen, W., & Ahmad, B. Bin. (2018). Landslide susceptibility mapping using J48 decision tree with adaboost, bagging and Rotation Forest ensembles in the Guangchang area (China). *Catena*, *163*, 399–413.

Huang, Y. F., Ang, J. T., Tiong, Y. J., Mirzaei, M., & Amin, M. Z. M. (2016). Drought Forecasting using SPI and EDI under RCP-8.5 Climate change scenarios for Langat River Basin, Malaysia. *Procedia Engineering*, *154*, 710–717.

Hussain, M., Yusof, K. W., Mustafa, M. R., & Afshar, N. R. (2015). Application of statistical downscaling model (SDSM) for long term prediction of rainfall in Sarawak, Malaysia. *WIT Transactions on Ecology and the Environment*, *196*, 269-278.

Kabiri, R., Ramani Bai, V., & Chan, A. (2013). Regional precipitation scenarios using a spatial statistical downscaling approach for Klang watershed , Malaysia. *Journal of Environmental Research And Development*, *8*(1), 126–134.

Kim, H. G., Lee, D. K., Park, C., Kil, S., Son, Y., & Park, J. H. (2015). Evaluating landslide hazards using RCP 4.5 and 8.5 scenarios. *Environmental Earth Sciences*, *73*, 1385–1400.

Lal, P. N., Mitchell, T., Aldunce, P., Auld, H., Mechler, R., Miyan, A., Romano, L. E., Zakaria, S., Dlugolecki, A., Masumoto, T., Ash, N., Hochrainer, S., Hodgson, R., Islam, T. U., Mc

Cormick, S., Neri, C., Pulwarty, R., Rahman, A., Ramalingam, B., … Wilby, R. (2012). National systems for managing the risks from climate extremes and disasters. In *Managing the risks of extreme events and disasters to advance climate change adaptation: Special report of the intergovernmental panel on climate change* (Vol. 9781107025). Cambridge University Press.

Lim, H. S., Jafri, M. Z. M., Abdullah, K., & Rajah, J. (2009). A case study of global warming in Penang Island, Malaysia. *IOP Conference Series: Earth and Environmental Science*, *6*, 412029.

Mahdaoui, K., & Asmlal, L. (2023). Downscaling future climate changes under RCP emission scenarios using CanESM2 climate model over the Bouregreg catchment, Morocco. *Modeling Earth Systems and Environment*, *9*, 2797-2807.

Malaysian Meteorological Department. (2009). Climate change scenarios for Malaysia 2001–2099.

Mavume, A. F., Banze, B. E., Macie, O. A., & Queface, A. J. (2021). Analysis of climate change projections for mozambique under the representative concentration pathways. *Atmosphere*, *12*(5), 588.

Moss, R. H., Edmonds, J. A., Hibbard, K. A., Manning, M. R., Rose, S. K., Van Vuuren, D. P., Carter, T. R., Emori, S., Kainuma, M., Kram, T., Meehl, G. A., Mitchell, J. F. B., Nakicenovic, N., Riahi, K., Smith, S. J., Stouffer, R. J., Thomson, A. M., Weyant, J. P., & Wilbanks, T. J. (2010). The next generation of scenarios for climate change research and assessment. *Nature*, *463*, 747–756.

Munawar, S., Rahman, G., Moazzam, M. F. U., Miandad, M., Ullah, K., Al-Ansari, N., & Linh, N. T. T. (2022). Future climate projections using SDSM and LARS-WG downscaling methods for CMIP5 GCMs over the Transboundary Jhelum River Basin of the Himalayas Region. *Atmosphere*, *13*(6), 898.

Munawar, S., Tahir, M. N., & Baig, M. H. A. (2021). Future climate change impacts on runoff of scarcely gauged jhelum river basin using SDSM and RCPS. *Journal of Water and Climate Change, 12(7)*, 2993–3004.

Mwabumba, M., Yadav, B. K., Rwiza, M. J., Larbi, I., Dotse, S. Q., Limantol, A. M., Sarpong, S., & Kwawuvi, D. (2022). Rainfall and temperature changes under different climate scenarios at the watersheds surrounding the Ngorongoro Conservation area in Tanzania. *Environmental Challenges*, *7*, 100446.

NAHRIM. (2013). Estimation of Future Design Rainstorm under the Climate Change Scenario in Peninsular Malaysia (Issue 1).

Noor, M., Ismail, T., Chung, E. S., Shahid, S., & Sung, J. H. (2018). Uncertainty in rainfall intensity duration frequency curves of Peninsular Malaysia under changing climate scenarios. *Water*, *10*(12), 1750.

Onarun, T., & Sittichok, K. (2023). Development of statistical downscaling methods for the assessment of rainfall characteristics under climate change scenarios Uncorrected Proof. *Journal of Water & Climate Change*, *14*(16), 2970-2987.

Onarun, T., Thepprasit, C., & Sittichok, K. (2023). Development of statistical downscaling methods for the assessment of rainfall characteristics under climate change scenarios. *Journal of Water and Climate Change, 14*(9), 2970-2987.

Pour, S. H., Harun, S. Bin, & Shahid, S. (2014). Genetic programming for the downscaling of extreme rainfall events on the east coast of peninsular Malaysia. *Atmosphere*, *5*(4), 914–936.

Protong, S., Carling, P. A., & Leyland, J. (2018). Climate change and landslide risk assessment in uttaradit province, Thailand. *Engineering Journal*, *22*(1), 243–255.

Rana, M., Adhikary, S., & Islam, M. (2023). Prediction of future temperature and precipitation changes in Bhola dstrict of Bangladesh using SDSM. 7th International Conference on Engineering Research, Innovation and Education, 12-14 January, Sylhet, Bangladesh.

Rana, M. M., & Adhikary, S. K. (2023). Climate change projection over southwest coastal region of Bangladesh using statistical downscaling model. *AIP Conference Proceedings, 2713*, 050016.

Raymond, P. L., Pabst, T., Bussière, B., & Bresson, É. (2020). Impact of climate change on extreme rainfall events and surface water management at mine waste storage facilities. *Journal of Hydrology, 590*, 125383.

Rianna, G., Zollo, A., Tommasi, P., Paciucci, M., Comegna, L., & Mercogliano, P. (2014). Evaluation of the effects of climate changes on landslide activity of Orvieto Clayey Slope. *Procedia Earth and Planetary Science, 9*, 54–63.

Robinson, P. J., & Finkelstein, P. L. (1991). The development of impact-oriented climate scenarios. *Bulletin - American Meteorological Society*, *72*(4), 481–490.

Sa'adi, Z., Alias, N. E., Yusop, Z., Chow, M. F., Muhammad, M. K. I., Mazilamani, L. S., Ramli, M. W. A., Shiru, M. S., Mohamad, N. A., Rohmat, F. I. W., & Khambali, M. H. M. (2024a). Spatiotemporal assessment of rainfall and drought projection for integrated dam management in Benut River Basin, Malaysia under CMIP6 scenarios. *Environmental Challenges, 15*, 100892.

Sa'adi, Z., Alias, N. E., Yusop, Z., Iqbal, Z., Houmsi, M. R., Houmsi, L. N., Ramli, M. W. A., & Muhammad, M. K. I. (2024b). Application of relative importance metrics for CMIP6 models selection in projecting basin-scale rainfall over Johor River basin, Malaysia. *Science of the Total Environment*, *912*, 169187.

Sa, Z., Eliza, N., Yusop, Z., Magdy, M., Shukla, P., Rajab, M., Athirah, N., Sanusi, M., Sa, N., Khairul, M., Muhammad, I., & Iqbal, Z. (2024). Characterization of the future northeast monsoon rainfall based on the clustered climate zone under CMIP6 in Peninsular Malaysia. *Atmospheric Research*, *304*, 107407.

Sammathuria, M. K., & Ling, L. K. (2009). Regional climate observation and simulation of extreme temperature and precipitation trends (pp. 1-9). IRCSA Conference, 3-6 Aug, Kuala Lumpur, Malaysia.

Siabi, E. K., Kabobah, A. T., Akpoti, K., Anornu, G. K., Amo-Boateng, M., & Nyantakyi, E. K. (2021). Statistical downscaling of global circulation models to assess future climate changes in the Black Volta basin of Ghana. *Environmental Challenges*, *5*, 100299.

Sørland, S. L., Schär, C., Lüthi, D., & Kjellström, E. (2018). Bias patterns and climate change signals in GCM-RCM model chains. *Environmental Research Letters, 13*(7), 074017.

Syafrina, A. H., Zalina, M. D., & Norzaida, A. (2017). Climate projections of future extreme events in Malaysia. A*merican Journal of Applied Sciences, 14*(3), 392–405.

Takhellambam, B. S., Srivastava, P., Lamba, J., Zhao, W., Kumar, H., Tian, D., & Molinari, R. (2024). Artificial neural network-empowered projected future rainfall intensity-duration-frequency curves under changing climate. *Atmospheric Research*, *297*, 107122.

Tan, M. L., Ibrahim, A. L., Yusop, Z., Chua, V. P., & Chan, N. W. (2017). Climate change impacts under CMIP5 RCP scenarios on water resources of the Kelantan River Basin, Malaysia. *Atmospheric Research*, *189*, 1–10.

Tang, K. H. D. (2019). Climate change in Malaysia: Trends, contributors, impacts, mitigation and

adaptations. *Science of the Total Environment, 650*(2), 1858–1871.

Tukimat, N. N. A., Ahmad Syukri, N. A., & Malek, M. A. (2019). Projection the long-term ungauged rainfall using integrated Statistical Downscaling Model and Geographic Information System (SDSM-GIS) model. *Heliyon*, *5*(9), e02456.

Van Vuuren, D. P., & Carter, T. R. (2014). Climate and socioeconomic scenarios for climate change research and assessment: reconciling the new with the old. *Climatic Change*, *122*, 415–429.

Van Vuuren, D. P., Stehfest, E., den Elzen, M. G. J., Kram, T., van Vliet, J., Deetman, S., Isaac, M., Klein Goldewijk, K., Hof, A., Mendoza Beltran, A., Oostenrijk, R., & van Ruijven, B. (2011). RCP2.6: exploring the possibility to keep global mean temperature increase below 2°C. *Climatic Change*, *109*, 95.

WHO. (2018). Climate Change and Health. World Health Organization Website. https://doi.org/10.17843/rpmesp.2016.331.2006

Wilby, R. L., & Dawson, C. W. (2007). SDSM 4.2— A decision support tool for th e assessment of regional climate change impacts, User Manual (pp. 1-94). Department of Geography, Lancaster University, UK.

Wilby, R. L., & Dawson, C. W. (2015). Statistical DownScaling Model-Decision Centric (SDSM-DC) Version 5.2 Supplementary Note 6 march 2015.

Wilby, R. L., Dawson, C. W., & Barrow, E. M. (2002). SDSM — A decision support tool for the assessment of regional climate change impacts. *Environmental Modelling & Software*, *17*(2), 145–157.

Yang, C. K., Shan, F. P., & Tien, T. L. (2020). Climate change detection in Penang island using deterministic interpolation methods. *Indonesian Journal of Electrical Engineering and Computer Science*, *19*(1), 412–419.

Yin, L. H., Ting, N. Y., Shan, F. P., Shimizu, K., & Lateh, H. (2019). Estimation of precipitation data by using deterministic interpolation methods: A case study in Penang Island. *AIP Conference Proceedings*, *2184*(1), 050018.

Zarei, Y., Khorshiddoust, A. M., Banafsheh, M. R., & Rostamzadeh, H. (2023). Assessing the impacts of global climate change on climate elements of temperature and precipitation in disparate climatic zones of Iran using RCP scenarios. *Journal of Geography and Planning*, *27*(83), 64–71.

Zhang, L. E. I., Xu, Y., Meng, C., Li, X., Liu, H., & Wang, C. (2020). Comparison of statistical and dynamic downscaling techniques in generating high-resolution temperatures in China from CMIP5 GCMs. *Journal of Applied Meteorology and Climatology*, *59*(2), 207–235.